$[^{99m}Tc(CO)_3]^+$ labeled histidine derivative containing 4-nitroimidazole: Synthesis, biodistribution as a tumor hypoxia imaging agent

MEI Lei CHU Taiwei*

Beijing National Laboratory for Molecular Sciences, *Radiochemistry and Radiation Chemistry Key Laboratory of Fundamental Science*, *College of Chemistry and Molecular Engineering*, *Peking University*, *Beijing 100871*, *China*

Abstract A novel histidine derivative containing 4-nitroimidazole, (S)-2-(4-((4-nitro-1H-imidazol-1-yl) methyl) benzamido) -3- (1H- imidazol-4-yl)propanoic acid (His-NI), was synthesized and labeled with $[^{99m}Tc(CO)_3(H_2O)_3]^+$. The tricarbonyl technetium complex, the $^{99m}Tc(CO)_3$-His-NI, showed a 99% yield under mild conditions at a low His-NI ligand concentration of 10^{-4} mol·L^{-1}, and its biodistribution in mice bearing S180 tumor had a selective accumulation in tumor (2.01±0.40 %ID/g at 1 h postinjection) and a slow clearance. The tumor/muscle ratio was 1.64 at 1 h, 3.10 at 4 h, and 3.88 at 24 h, indicating that the $^{99m}Tc(CO)_3$-His-NI has a potential to image tumor hypoxia.

Key words Tumor, Hypoxia, 4-nitroimidazole, $[^{99m}Tc(CO)_3(H_2O)_3]^+$, Histidine

1 Introduction

Hypoxic tumor tissues are resulted from mismatching vasculature angiogenesis. They surround the growing tumor, and absorb radiations, affecting clinic outcomes of the radiotherapy[1]. Therefore, the tumor hypoxia identification and quantification are important in predicting a treatment effect[2,3], and nuclear medicine can be of help in revealing the tumor hypoxia. Nitroimidazole-based radiopharmaceuticals, with their favorable pharmacokinetics and properties, have been studied to selectively target tumor hypoxia [4–6]. In hypoxic tissues, nitro groups of nitroimidazoles are reduced by enzymatic catalysis of nitroreductase, decomposed into radicals, bound to cellular macro molecules and trapped in hypoxic cells. In normal cells, the nitroimidazole is re-oxidized to its original form by oxygen after enzymatic reductions[7–9]. ^{18}F-FMISO and ^{123}I-IAZA containing 2-nitroimidazole are promising radiopharmaceuticals to detect hypoxia [10,11], but they are expensive, with limited availability [12]. A better alternative is to use ^{99m}Tc- labeled agents, which are convenient to prepare. While the 2-nitro-imidazole derivatives were extensively studied, the 4-nitro- and 5-nitroimidazole derivatives were explored as imaging agents[13,14].

In ^{99m}Tc-based complexes, the ^{99m}Tc(V) oxo core is commonly used, but it is disadvantageous with its multi-step synthesis of ligand, low specific activity and large size. Generally, the novel technetium cores applicable for labeling are oxidation-stable and easily accessible precursor. A promising drug to label a variety of ligands is organometallic $[^{99m}Tc(CO)_3 \cdot (H_2O)_3]^+$[15–17], which is less oxidation- sensitive, with substitutionally labile ligand of three water molecules and high affinity to a large variety of ligands, such as 2-picolyl- amine- *N*,*N*-diacetic acid, histidine, imino-diacetic acid etc. Recently, Mallia *et al.*[18,19] isolated and evaluated an unsubstituted 5-nitroimidazole derivative with an iminodiacetic acid group, and compared the hypoxia- targeting potential of $^{99m}Tc(CO)_3$-labeled imino- diacetic acid derivatives of 2-nitro and 4-nitro- imidazoles. But histidine-modified nitro- imidazole as a hypoxia-targeting agent has not been known yet. It is reported that histidine derivatives are potent ligands with high specific activities and stabilities[20,21], and a histidine derivative containing

Supported by the National Natural Science Foundation of China (Grant No. 20771011 and 21071010).

* Corresponding author. *E-mail address:* twchu@pku.edu.cn

Received: 2010-12-15

4-nitroimidazole may serve as a ligand for tricarbonyl technetium and a tumor hypoxia imaging agent.

In this study, a new histidine derivative containing 4-nitroimidazole, (S)-2-(4-((4-nitro- 1H-imidazol-1-yl) methyl) benzamido)-3-(1H-imidazol-4-yl)propanoic acid (His-NI), was synthesized, and labeled with $[^{99m}Tc(CO)_3(H_2O)_3]^+$ to prepare the $^{99m}Tc(CO)_3$-His-NI as a tumor hypoxia imaging agent. Stability of the $^{99m}Tc(CO)_3$-His-NI was studied, and its biodistribution *in vivo* was evaluated.

2 Materials and Methods

The 4-nitroimidazole (98%) was purchased from Acros Organics. L(+)-histidine methyl ester dihydrochloride (H-His-OMe·2HCl) (>98%) and benzotriazole-1-yl-oxy-tris-(dimethylamino)-phosphonium hexafluorophosphate (BOP) (>98%) were from GL Biochem. N-bromosuccinimide (NBS) was re-crystallized from water. Carbon tetrachloride, acrylonitrile and triethylamine were purified by distillation. All other reagents (AR grade) were used as received. The $^{99m}TcO_4^-$ was eluted from a ^{99}Mo-^{99m}Tc generator (China Institute of Atom Energy, Beijing) using saline. Murine sarcoma S180 cell line was provided by College of Life Sciences, Peking University. Kunming mice (20–25 g, male) were supplied by Breeding Center of the Institute of Zoology, Chinese Academy of Sciences.

^1H NMR spectra were recorded on a Varian Mercury Plus (300 MHz) and a Bruker ARX-400 (400 MHz) spectrometer using deuterated dimethyl sulfoxide (DMSO-d_6) or chloroform ($CDCl_3$) as a solvent, and tetramethylsilane (TMS) as an internal standard. Electron impact mass spectra (EI-MS) were obtained with a ZAB-HS mass spectrometer (Micromass), and ESI-MS spectra were obtained with a Finnigan LCQ Deca XP Plus ion trap mass spectrometer (Thermo Finnigan). Radioactivity of mice organs or tissues was assayed using a Cobra II series Auto-Gamma Counting System (Packard). The HPLC analysis was performed with a reversed-phase column (Agilent HC-C18, 4.6 ×150 mm, 5 μm), a Waters 2487 dual wavelength absorbance detector (waters 600E series), and a radiometric detector (Packard 500TR series) system. The 0.1% trifluoroacetic acid (solvent A) and methanol (solvent B) were used as the gradient system (0–3 min, 100% A; 3–25 min, 100–0% A; 25–30 min, 0% A; 30–33 min, 0–100% A).

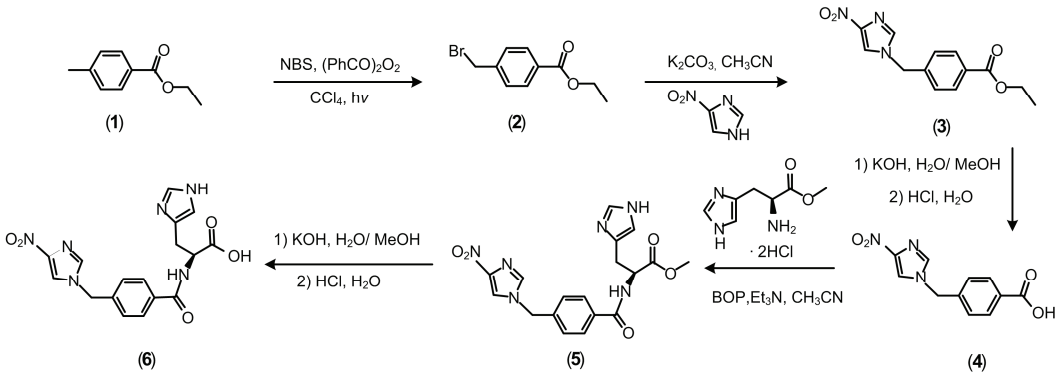

Scheme 1 Synthesis of histidine derivative of 4-nitroimidazole, (**6**).

2.1 The synthesis

His-NI containing histidine was synthesized by five steps, as illustrated in Scheme 1. Ethyl 4-(bromomethyl) benzoate in CCl_4 was brominated by using NBS under the light presence, and the crude ethyl 4-(bromomethyl) benzoate reacted with 4-nitroimidazole in K_2CO_3 acetonitrile solution. After hydrolysing and acidifying product **3**, product **4** was obtained and confirmed by the ^1H-NMR, and it was coupled with the amino group of histidine methyl ester by amide linkage. Finally, the target product **6** with two chelating sites was obtained by hydrolysing the carbomethoxy to coordinate with tricarbonyl technetium.

2.1.1 Ethyl 4-((4-nitro- 1H-imidazol- 1-yl) methyl) - benzoate (3)

Benzoyl peroxide (32.0 mg, 0.132 mmol) was added into the ethyl 4-methylbenzoate (**1**) (1.66 g, 10.1 mmol)

in dry carbon tetrachloride (20 mL). The mixture was stirred and refluxed under UV light. N-bromo-succinimide (NBS; 1.90 g, 10.6 mmol) was added in two portions with a time interval of 30 min, the mixture was stirred for 4 h under reflux, and separated by hot filtering. The filtrate was distilled under reduced pressures, and the crude bromide (**2**) as light yellow oil was obtained, with a yield rate of 44% (1.07 g). The anhydrous potassium carbonate (0.56 g, 4.00 mmol) was added into 4-nitroimidazole (0.45 g, 4.00 mmol) in acetonitrile (15 mL) and stirred for 30 min to form a yellow emulsion. The product **2** (1.07 g, 4.10 mmol) in acetonitrile (15 mL) was added and refluxed overnight. After cooled down and filtration, the filtrate was evaporated into a yellow residue, purified by chromatography on a silica gel column, and eluted with dichloromethane to give a white ethyl 4-((4-nitro-1H-imidazol-1-yl)methyl)-benzoate (**3**) (0.58 g , 53%).

^{1}H-NMR (300 MHz, $CDCl_3$, δ ppm): 8.11 (2H, m, phenyl C_2-H); 7.73 (1H, s, imidazole C_5-H); 7.51 (1H, s, imidazole C_2-H); 7.28 (2H, m, phenyl C_3-H); 5.24 (s, 2H, phenyl-CH_2); 4.40 (q, 2H, -$COOCH_2$); 1.40 (t, 3H, -CH_3). EI-MS calculated for $C_{13}H_{13}O_4N_3$ (M^+): *m*/*z* 275. Found: 275.

2.1.2 4-((4-nitro-1H-imidazol-1-yl) methyl)-benzoic acid (4)

The product **3** (0.58 g, 2.11 mmol) in methanol (3 mL) was added into KOH aqueous solution (10 mL; 0.22 g, 3.93 mmol) and stirred at about 60ºC. The hydrolysis was monitored by TLC (AcOEt as developing solvent). After the reaction, the mixture was cooled to room temperature, and acidified to pH~2 with 6 mol·L^{-1} HCl, to yield the product **4**, a light yellow 4,4-((4-nitro-1H-imidazol-1-yl)methyl)-benzoic acid (0.43 g, 82%).

^{1}H-NMR (300 MHz, d_6-DMSO, δ ppm): 8.52 (1H, s, imidazole C_5-H); 8.02 (1H, s, imidazole C_2-H); 7.95 (2H, m, phenyl C_2-H); 7.45 (2H, m, phenyl C_3-H); 5.41 (s, 2H, phenyl-CH_2). EI-MS calculated for $C_{11}H_9O_4N_3$ (M^+): *m*/*z* 247. Found: 247.

2.1.3 (S)-methyl 2-(4-((4-nitro-1H-imidazol-1-yl) methyl) benzamido)-3-(1H-imidazol -4-yl) propanoate (5)

Triethylamine (0.71 g, 7.02 mmol) and BOP (0.88 g, 2.00 mmol) were added into product **4** (0.50 g, 2.02 mmol) in acetonitrile (20 mL), and stirred for 30 min at room temperature, thus forming a brownish yellow solution. Then L(+)-histidine methyl ester dihydrochloride (0.53 g, 2.19 mmol) was added and stirred at 35ºC overnight. After the solvent was evaporated under reduced pressures, the crude residue was washed by deionized water (2×20 mL) and recrystallized by methanol/H_2O (2/1) to obtain product **5**.

^{1}H-NMR (400 MHz, d_6-DMSO, δ ppm): 8.49 (1H, s, nitroimidazole C_5-H); 8.00 (1H, s, nitro-imidazole C_2-H); 7.87 (1H, s, His imidazole C_2-H); 7.83 (2H, m, phenyl C_2-H); 7.47 (2H, m, phenyl C_3-H); 6.98 (1H, s, His imidazole C_5-H); 5.38 (2H, s, phenyl-CH_2); 4.70 (1H, m, N-CH-COO); 3.63 (3H, s, $COOCH_3$); 3.09 (2H, m, His imidazole-CH_2). ESI-MS calculated for $C_{18}H_{18}N_6O_5$ (M^+): *m*/*z* 398.1. Found: 399.1 $(M+H)^+$.

2.1.4 (S)-2-(4-((4-nitro-1H-imidazol-1-yl) methyl) benzamido)-3-(1H-imidazol -4-yl)propanoic acid (His-NI) (6)

Product **5** (0.10 g, 0.25 mmol) in methanol (1 mL) was added with 10 eq of 2 mol·L^{-1} KOH (0.14 g, 2.5 mmol). The mixture was stirred for 30 min at 60^{o}C, cooled to room temperature, and acidified to pH~2 with 6 mol·L^{-1} HCl, yielding product **6**, a brownish His-NI solid (0.08 g, 83%).

^{1}H-NMR (400 MHz, d_6-DMSO, δ ppm): 9.00 (1H, s, His imidazole C2-H); 8.52 (1H, s, nitro-imidazole C_5-H); 8.03 (1H, s, nitroimidazole C_2-H); 7.86 (2H, m, phenyl C_2-H); 7.46 (2H, m, phenyl C_3-H); 7.41 (1H, s, His imidazole C_5-H); 5.38 (2H, s, phenyl-CH_2); 4.75 (1H, m, N-CH-COO); 3.24 (2H, m, His imidazole-CH_2). ESI-MS calculated for $C_{17}H_{16}N_6O_5$ (M^+): *m*/*z* 384.1. Found: 385.1 $(M+H)^+$.

2.2 Radiolabeling

$[^{99m}Tc(CO)_3(H_2O)_3]^+$ precursor was prepared according to the modified procedure reported in Ref. [15]. After a saline solution (0.5 mL) of sodium borohydride (5 mg), sodium carbonate (5 mg) and Na/K tartrate (15 mg) in a sealed penicillin vial was purged with carbon monoxide for 5 min, the 1-mL pertechnetate (37–74 MBq) was added using a syringe, and heated at 75ºC for 30 min. The cooled mixture was neutralized using 1 mol·L^{-1} HCl, and analyzed by HPLC. The precursor yield was >99%.

The His-NI solution (100 μL, 1.0 mg·mL^{-1}) was mixed with the freshly prepared [^{99m}Tc(CO)$_3$·(H$_2$O)$_3$]$^+$ (400 μL, ~37 MBq), and diluted with 500-μL phosphate buffer (pH 7.2, 0.1 mol·L^{-1}). Vortexed for 5 min, the mixture was heated at 75ºC for 1 h, and ^{99m}Tc(CO)$_3$-His-NI was prepared.

2.3 Partition coefficient and stability

Partition coefficient was determined as reported previously[22,23]. The 1-octanol (1 mL) was added to a mixture of 0.9-mL water and 0.1-mL radiolabeling complex, and votexed for 5 min at room temperature. The mixture was centrifuged at 4000 rpm for 5 min, and equal aliquots (100 μL) for each phase were used to count the radioactivity. The partition coefficient was obtained by dividing the radioactivity of the octanol and the water layers. The aqueous layer measurement was repeated three times.

After preparation, the ^{99m}Tc(CO)$_3$-His-NI was incubated at 37ºC, and certain aliquots at different time were taken for HPLC analysis. According to the procedure reported in Ref.[17], the competition experiment histidine in the ^{99m}Tc(CO)$_3$-His-NI was conducted. The histidine solution (900 μL; 0.001 mol·L^{-1}) in phosphate buffer (0.1 mol·L^{-1}, pH 7.2), and the newly prepared [^{99m}Tc(CO)$_3$(H$_2$O)$_3$]$^+$ (100 μL) were added. After complete mixing, the mixture was incubated at 37°C and analyzed by HPLC at 1 and 4 h after incubation.

2.4 Biodistribution

Sarcoma tumor (S180) was grown in male Kunming mice by hypodermically injecting about 10^6 S180 cells into the left front leg. The tumor growth rate was 10–15 mm in size (or 0.5–1.5 g) per week. The mice bearing S180 tumor of 20–25 g were injected via the tail vein using the freshly prepared ^{99m}Tc(CO)$_3$-His-NI (100 μL, 0.6 MBq) with a total His-NI ligand concentration of 1.0×10^{-4} mol·L^{-1}, and sacrificed in five groups at various time intervals. The organs and tissues of interest were removed, washed, and weighed in plastic tubes to count the radioactivity on the auto gamma counting system. The uptake of tissue per gram was calculated as percentage of the total injection dose (% ID/g) using its standard equivalent to 1%. The data were expressed in mean ± S.D. Tumor/relevant tissue ratios were calculated from % ID/g. All experiments accorded with the principles of laboratory animal care and the China law on the animal protection.

3 Results and Discussion

3.1 Radiolabeling

The [^{99m}Tc(CO)$_3$(H$_2$O)$_3$]$^+$ was prepared as reported previously[15], and determined by C_{18} reversed phase HPLC, indicating that a characteristic broad peak at 7.80 min was distinguished from that of pertechnetate at 2.70 min. The ^{99m}Tc(CO)$_3$-His-NI was prepared by incubating His-NI with [^{99m}Tc(CO)$_3$(H$_2$O)$_3$]$^+$ at 75 °C and pH 7.2 for 1 h. The resultant ^{99m}Tc(CO)$_3$-His-NI with yield of >99% has a single sharp peak at 16.60 min at a low His-NI ligand concentration of 1.0×10^{-4} mol·L^{-1} (Fig.1), and is comparable to that of Ref.[17].

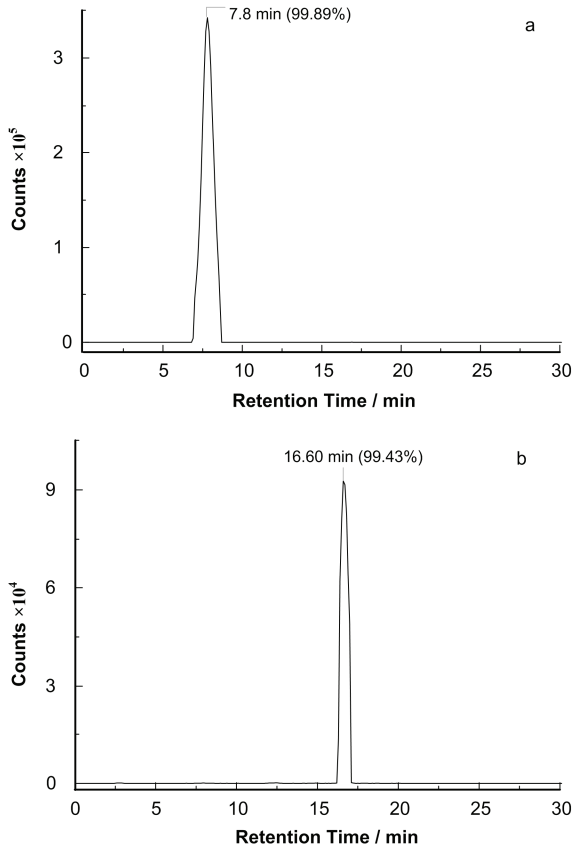

Fig.1 HPLC analysis of ^{99m}Tc(CO)$_3$(H$_2$O)$_3$]$^+$ precursor(a) and ^{99m}Tc(CO)$_3$-His-NI complex(b).

The partition coefficient (log $P_{o/w}$) of the ^{99m}Tc(CO)$_3$-His-NI was determined as –1.08 ± 0.02, indicating that it was of low lipophilicity. It was stable during 4 h in PBS (pH 7.2) at 37ºC, with the sharp

peak at 16.60 min for the 1 and 4 h HPLC measurements, but no peak at 11.90 min corresponding to $^{99m}Tc(CO)_3$-histidine complex was observed.

3.2 Biodistribution

Table 1 shows the biodistribution of $^{99m}Tc(CO)_3$-His-NI in mice bearing S180 tumor. The tumor uptake was 2.01 ± 0.40 % ID/g at 1 h, and declined slowly from 4 to 24 h. The retention data in blood were 4.16 ± 0.28 %ID/g at 1 h, 3.66 ± 0.26 % ID/g at 4 h, and 1.09 ± 0.36 % ID/g at 24 h, showing the slow clearance. The tumor/blood ratio kept almost the same from 1 to 8 h, but it was 0.62±0.05 at 24 h. The tumor/muscle ratios were 1.64 at 1 h and 3.10 at 4 h, but increased slightly from 8 to 24 h. The results are similar to the hypoxia-imaging agent of BMS181321[26] in other tumor models. However, the $^{99m}Tc(CO)_3$-His-NI with low lipophilicity had high liver radioactivity at 4 h. This may be attributed to its slow clearance from blood. The radio-activity in liver and kidney reflected its urinary and hepatic eliminations.

Table 1 Biodistribution of $^{99m}Tc(CO)_3$-His-NI in mice bearing S180 tumor (%ID/g)*.

Tissues	1 h	4 h	8 h	24 h
Blood	4.16±0.28	3.66±0.26	1.87±0.04	1.09±0.36
Brain	0.23±0.07	0.09±0.02	0.10±0.04	0.04±0.01
Muscle	1.09±0.17	0.45±0.03	0.25±0.01	0.20±0.04
Heart	3.38±0.37	1.05±0.08	0.80±0.20	0.51±0.17
Spleen	9.23±2.52	4.88±1.60	3.37±0.67	1.55±0.18
Lung	15.48±3.04	6.58±1.19	3.41±0.23	3.83±1.15
Stomach	7.44±0.66	3.43±0.41	1.54±0.63	0.72±0.27
Kidney	13.02±1.84	7.16±1.41	4.33±0.24	4.74±0.33
Intestine	6.22±1.10	1.44±0.15	0.83±0.06	0.48±0.12
Liver	28.58±3.92	20.48±2.09	9.78±0.83	11.08±3.36
Tumor	2.01±0.40	1.45±0.15	0.99±0.24	0.70±0.19
Tumor/blood	0.44±0.04	0.40±0.04	0.44±0.02	0.62±0.05
Tumor/muscle	1.64±0.35	3.10±0.44	3.18±0.24	3.88±0.25

* That data are expressed in mean ± S.D.

Table 2 shows the $P_{o/w}$ values, tumor/muscle and tumor/blood ratios of $^{99m}Tc(CO)_3$-His-NI and other tumor hypoxia markers at 1 h postinjection. Its tumor/blood ratio is similar with iminodiacetic acid derivatives of nitroimidazole (IDA-n-NI), but lower than that of N4IPA, N2IPA and HL91, and higher than that of ^{99m}Tc-BMS181321, a popular hypoxia-imaging agent. Also, its tumor/muscle ratio is lower than of other hypoxia markers proposed.

Table 2 $P_{o/w}$ value, tumor/muscle and tumor/blood ratios of $^{99m}Tc(CO)_3$-His-NI, and other tumor hypoxia markers at 1 h postinjection.

Label	Ligand	$P_{O/W}$	Tumor/muscle	Tumor/blood	Tumor model	References
$[^{99m}Tc(CO)_3]^+$	His-4-NI	0.08	1.64	0.44	S180	This work
$[^{99m}Tc(CO)_3]^+$	IDA-5-NI	0.15	3.60	0.37	Fibrosarcoma	[18,24]
$[^{99m}Tc(CO)_3]^+$	IDA-4-NI	0.14	3.50	0.58	Fibrosarcoma	[19]
$[^{99m}Tc(CO)_3]^+$	IDA-2-NI	0.13	2.38	0.49	Fibrosarcoma	[19]
$[^{99m}TcO]^{3+}$	N4IPA	—	4.25	1.19	S180	[14]
$[^{99m}TcO]^{3+}$	N2IPA	0.04	2.50	0.71	S180	[25]
$[^{99m}TcO]^{3+}$	BMS181321	40	2.72	0.22	KHT	[26]
$[^{99m}TcO]^{3+}$	HL-91	0.10	4.00	1.40	KHT	[27]

4 Conclusions

The His-NI was synthesized and labeled with $[^{99m}Tc(CO)_3(H_2O)_3]^+$ at a low His-NI ligand concentration of 10^{-4} mol·L^{-1}. Biodistribution in mice bearing S180 tumor demonstrated a selective tumor accumulation with a moderate tumor/muscle and tumor/blood ratios. The $^{99m}Tc(CO)_3$-His-NI with a slow blood clearance from may limit its hypoxia imaging performance, similar to iminodiacetic acid

derivatives of nitroimidazole. It is underway to make further modification as a novel hypoxia imaging agent.

References

1 Brown J M, Giaccia A J. Cancer Res, 1998, **58:** 1408–1416.

2 Chapman J D, Engelhardt E L, Stobbe C C, *et al.* Radiother Oncol,1998, **46:** 229–237.

3 Vaupel P, Mayer A. Cancer Metastasis Rev, 2007, **26:** 225–239.

4 Nunn A, Linder K, Strauss H W. Eur J Nucl Med, 1995, **22:** 265–280.

5 Linder K E, Chan Y W, Cyr J E. *et al.* J Med Chem, 1994, **37:** 9–17.

6 Xu H, Chu T W, Wang X Y, *et al.* Appl Radiat Isot, 2005, **62:** 919–922.

7 Edwards D I. J Antimicrob Chemoth, 1993, **31:** 9–20.

8 Edwards D I. J Antimicrob Chemoth, 1993, **31:** 201–210.

9 Hodgkiss R J. Anti-Cancer Drug Des, 1998, **13:** 687–702.

10 Grunbaum Z, Freauff S J, Krohn K A, *et al.* J Nucl Med, 1987, **28:** 68–75.

11 Mannan R H, Somayaji V V, Lee J, *et al.* J Nucl Med, 1991, **32:** 1764–1770.

12 Ballinger J R. Semn Nucl Med, 2001, **31:** 321–329.

13 Das T, Banerjee S, Samuel G, *et al.* Nucl Med Biol, 2003, **30:** 127–134.

14 Chu T W, Hu S W, Wei B, *et al.* Bioorg Med Chem Lett, 2004, **14:** 747-749.

15 Alberto R, Schibli R, Egli A, *et al.* J Am Chem Soc, 1998, **120:** 7987–7988.

16 Alberto R, Schibli R, Waibel R, *et al.* Coord Chem Rev, 1999, **192:** 901–919.

17 Schibli R, La Bella R, Alberto R, *et al.* Bioconjugate Chem, 2000, **11:** 345–351.

18 Mallia M B, Subramanian S, Mathur A, *et al.* Bioorg Med Chem Lett, 2008, **18:** 5233–5237.

19 Mallia MB, Subramanian S, Mathur A, *et al.* J Label Compd Radiopharm,2008, **51:** 308–313.

20 Egli A, Alberto R, Tannahill L, *et al.* J Nucl Med, 1999, **40:** 1913–1917.

21 Garcia-Garayoa E, Allemann-Tannahill L, Blauenstein P, *et al.* Nucl Med Biol, 2001, **28:** 75–84.

22 Li Z J, Chu T W, Liu X Q, *et al.* Nucl Med Biol, 2005, **32:** 225–231.

23 Chu T W, Xu H, Yang Z, *et al.* Appl Radiat Isot, 2009, **67:** 590–593.

24 Mallia M B, Subramanian S, Banerjee S, *et al.* Bioorg Med Chem, 2006, **14:** 7666–7670.

25 Chu T W, Li R J, Hu S W, *et al.* Nucl Med Biol, 2004, **31:** 199–203.

26 Ballinger J R, Kee J W M, Rauth A M, *et al.* J Nucl Med, 1996, **37:** 1023–1031.

27 Zhang X, Melo T, Ballinger J R, *et al.* Int J Radiat Oncol, 1998, **42:** 737–740.